



Showcasing research from Professor Jurriaan Huskens' laboratory, MESA+ Institute & Faculty of Science & Technology, University of Twente, Enschede, The Netherlands.

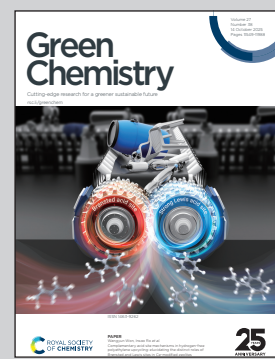
Polyurethane depolymerization by dialkyl carbonates: toward sustainable chemical recycling

A chemical route has been developed to depolymerize polyurethane foams into their monomeric units, providing high yields of both the aromatic and the polyol constituents. The use of diethyl carbonate provides these monomers as the carbamates and carbonates, respectively, and allows the implementation of the chemistry into a green recycling process that avoids the use of phosgene.

Image reproduced by permission of Ege Hosgor and Selena Deger from *Green Chem.*, 2025, **27**, 11782.

Artwork created by Ege Hosgor and Selena Deger, modified using Google Gemini.

## As featured in:



See Jean-Paul Lange, Jurriaan Huskens *et al.*, *Green Chem.*, 2025, **27**, 11782.



Cite this: *Green Chem.*, 2025, **27**, 11782

## Polyurethane depolymerization by dialkyl carbonates: toward sustainable chemical recycling

Ege Hosgor, Ricardo P. Martinho, Jip S. Hoogland, <sup>a</sup> Yuqi Jia, <sup>a</sup> Anahi Morales Gomez, <sup>a</sup> Willem Verboom, Jean-Paul Lange <sup>\*b</sup> and Jurriaan Huskens <sup>\*a</sup>

Polyurethane foams (PUFs), a major component of common consumer products such as mattresses, generally end up in landfills because they cannot be properly recycled. As thermoset, PUFs cannot be remolten to new products either. As condensation polymer, they can be depolymerized to recover one monomer, the polyol, but generally not the diisocyanate co-monomer without using phosgene, a toxic and wasteful reagent. We show here the possibility to depolymerize PUF in a way that enables a harmless, waste-free and phosgene-free recovery of both diisocyanate and polyol. Accordingly, the PUF is depolymerized with a dialkyl carbonate – providing carbonyl exchange at low concentrations of nucleophile – to deliver a carbonated polyol with 90% yield and aromatic dicarbamates with 70% yield under non-optimized conditions. These precursors are known to be converted to the original polyols and diisocyanates at high yield by alcoholysis and pyrolysis, respectively. We present advanced analytical methods to characterize and quantify the depolymerization products. We also report model reactions to show that the depolymerization proceeds through a thermodynamic equilibration of carbonates, carbamates and ureas.

Received 21st May 2025,

Accepted 13th August 2025

DOI: 10.1039/d5gc02533h

rsc.li/greenchem

### Green foundation

1. This work introduces a novel approach to depolymerize polyurethane (PU) foams and recover both constituents, the polyols and diisocyanates, without using phosgene that is very toxic and wasteful.
2. Our approach offers a greener alternative by minimizing reagent toxicity and waste generation. The process replaces toxic phosgene reagent with bio-based diethyl carbonate. It also avoids the release of  $\text{Cl}^-$  waste and includes the recycling of EtOH back to DEC. Without full optimization, the method achieves recovery of up to 70% of the aromatic monomer and 80% of the polyol, highlighting both its efficiency and potential for circular recovery of PU building blocks.
3. Future improvements should include efficient recovery of solvent and catalyst, efficient separation of monomers and detailed process research.

## Introduction

Thermoset polymers such as polyurethanes (PUs) are widely used in applications like foams, elastomers, coatings, adhesives and fibers; however, they also cause significant waste, highlighting the need for carefully designed recycling processes.<sup>1–4</sup> The global market for PU is projected to expand from 24 million tons in 2020 to 31 million tons by 2030, driven by growth in demand for mattresses and furniture, and in electronics, automotive, and construction.<sup>5</sup> Flexible poly-

urethane foam (PUF) is a highly demanded material owing to its light weight and durability.<sup>6</sup> Industrial PUFs are synthesized through the polyaddition reaction between two key components, generally aliphatic polyols ( $\text{R(OH)}_3$ ) and aromatic or aliphatic diisocyanates ( $\text{O=C=N-R-N=C=O}$ ), yielding crosslinked polymers with urea and carbamate linkages ( $-\text{O-C(O)-NH-}$  and  $-\text{NH-C(O)-NH-}$ ).<sup>7</sup> Polyols vary in structure, weight, and functionality, all of which influence the final material properties. About 80% of the market is occupied by polyether polyols, mainly poly(propylene oxide)-poly(ethylene oxide) copolymers and poly(tetramethylene ether) glycols.<sup>8</sup> The remaining 20% are polyester polyols. While polyester polyols provide better mechanical strength, polyesters are more common due to their lower cost and greater hydrolytic stability.<sup>8,9</sup>

Since PUFs are thermoset polymers, they are chemically cross-linked and cannot be recycled mechanically, *i.e.*, by re-

<sup>a</sup>Department for Molecules & Materials, MESA+ Institute and Faculty of Science & Technology, University of Twente, P.O. Box 217, 7500 AE Enschede, The Netherlands.  
E-mail: [j.huskens@utwente.nl](mailto:j.huskens@utwente.nl)

<sup>b</sup>Sustainable Process Technology Group, Faculty of Science & Technology, University of Twente, P.O. Box 217, 7500 AE Enschede, The Netherlands.  
E-mail: [j.p.lange@utwente.nl](mailto:j.p.lange@utwente.nl)



melting and re-processing.<sup>10</sup> Therefore, large amounts of PUFs currently end up in landfills or incineration.<sup>11</sup>

To enable a complete chemical recycling of PUF waste and to obtain closed-loop production and recycling of PU, it is critical to recover both polyols and aromatic diisocyanates. Currently as comprehensively illustrated by Skrydstrup *et al.*,<sup>12</sup> alcoholysis, hydrolysis, acidolysis and aminolysis for deconstruction of PU materials result in a mixture composed of polyols and different aromatic amines.<sup>12–19</sup> The prime mechanistic reason for the formation of aromatic amines is that all methods use a process of exchange of nucleophiles at a carbonyl center and do so at high excess of nucleophile (*i.e.*, alcohol, water, amine). From the perspective of aromatic recovery, the formation of diamines results in their subsequent loss. Even when the diamines would be isolated, their conversion to diisocyanate requires the use of phosgene, which is highly toxic, requires much energy for manufacture and delivers much Cl waste upon use.<sup>20</sup> Due to the virgin-like properties such as functionality, molar mass and purity of the original polyols, remaining a significant obstacle to overcome.<sup>21</sup> Moreover, these depolymerization processes require a high energy input, which restricts their industrial use.<sup>22,23</sup> Overall, these methods primarily facilitate the recovery of the polyols, thereby enabling a certain degree of recycling of PUFs, but the recovery of the aromatics remains problematic.<sup>24,25</sup> The use of phosgene can be avoided when the aromatics would be recovered as carbamates,<sup>26</sup> as earlier work has shown that aromatic carbamates can be converted directly into isocyanates.<sup>27</sup> Essential is then to recover the aromatics in some carbonylated form, not as free nucleophiles obtained by nucleophilic depolymerization discussed above.

Diethyl carbonate (DEC) plays a key role in development of sustainable polymers. It can be synthesized from bioethanol and captured CO<sub>2</sub>, making it a renewable, low-toxicity, and biodegradable reagent.<sup>28–31</sup> These features align well with green chemistry principles, and its use supports the development of more sustainable recycling strategies for PU materials.

Here, we present a depolymerization method that employs carbonyl exchange to recover the polyols and convert aromatic components into aromatic dicarbamates, which can be thermally cleaved to diisocyanates without needing the hazardous phosgene.<sup>27</sup> As a proof of concept, we employ DEC both as depolymerization reagent and solvent. Our main objective is to evaluate the product distribution upon PUF depolymerization and to assess whether an equilibrium reaction between carbamate, urea, and carbonate derivatives (Fig. 1a) is established. Essential in this scheme is the avoidance of nucleophiles to prevent the liberation of free amines. Surprisingly, this approach leads to spontaneous separation of the polyols and carbamates, which greatly facilitates their separate workup and processing. We also report on the depolymerization of the model compounds 1,3-diphenyl urea (DPU) and ethyl *N*-phenyl carbamate (EPC) to demonstrate the equilibrium between urea and carbamate linkages, which are both present in PUF networks. We investigated the depolymerization catalysts by varying the catalyst composition, optimizing its loading, and

exploring routes for its recycling and reactivation. In all cases the reaction products were analyzed by <sup>1</sup>H NMR and quantified with qNMR spectroscopy.

## Results and discussion

### Depolymerization of PUF with diethyl carbonate

As a prime illustration of the concept, we successfully depolymerized commercial PUF in DEC with zinc acetate as a catalyst (procedure described in Experimental section), facilitating the carbonyl exchange reaction between the carbonate and the urea and carbamate linkages present in the PUF network. We used a commercially available flexible PUF, provided by Shell, which contains typical additives and reflects real PUF formulations (see SI for detailed composition and analyses). The foam is based on a TDI-polyether system with a TDI isomer ratio of 80 : 20 (2,4 : 2,6 isomers) and exhibits characteristic urethane and urea linkages, as confirmed by FTIR analysis. Elemental analysis (C/N/O) further supports its composition. By using this industrially relevant material, the applicability of this work is beyond idealized model systems.

In Fig. 1a, a full-cycle process is shown envisioning to recycle both the polyol and the aromatic component. The polymer undergoes a depolymerization with the excess DEC to recover both the polyol and the aromatic monomers. We assume this process to occur through a chemical equilibration between carbonyl compounds, ureas, carbamates and carbonates,<sup>32</sup> as is presented in Fig. 1b and which will be demonstrated below. As illustrated in Fig. 1c, PUF (0.4 g, composition shown in Table S1) and catalyst (typically zinc acetate) are suspended in 20 mL DEC and heated at 210 °C in an autoclave for 4 h. Afterwards, the reaction mixture is filtered to separate off the remaining solid (which contains leftover polymer and other non-soluble species), the excess DEC is evaporated from the liquid phase, both filtered solid and DEC-free filtrate are weighed individually. After the depolymerization, we observed a suspension of 0.03 g solid with 0.4 g oily liquid. Our experiments demonstrated the successful depolymerization, as evidenced by a good recovery of monomeric constituents in the liquid phase (analysis discussed below) and a minimal residue remaining in the solid phase.

The PUF depolymerization by DEC yields both the polyol and the aromatic monomers with high yield. We quantified the monomer yields of the depolymerization in the liquid phase using qNMR spectroscopy, integrating the signals of the characteristic protons from both monomers and comparing them to those of the synthesized dicarbamates (2,4- and 2,6-toluene dicarbamates, 2,4-/2,6-TDC) as well as the functionalized polyol (see a detailed explanation of the quantification in the SI). The <sup>1</sup>H NMR analysis of individually tested additives in PUF formulation confirmed that their peaks did not overlap with those of the main compounds, ensuring clear spectral distinction. Fig. 2a shows the chemical structures of all the main possible depolymerization products. The <sup>1</sup>H NMR spectrum of the depolymerization crude (Fig. 2b) shows that both



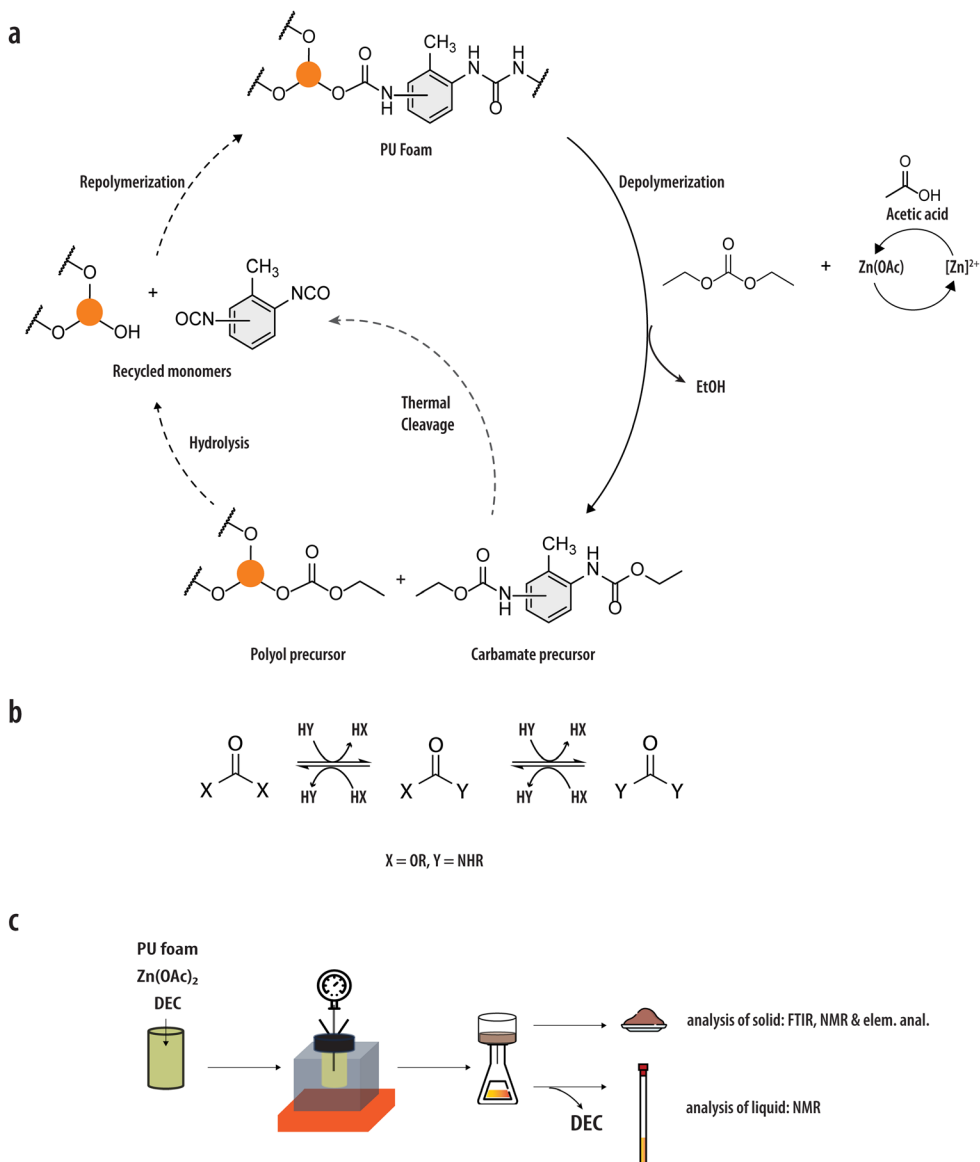


**Fig. 1** Overview of the full chemical recycling process: (a) conceptual representation of the depolymerization of PUF with diethyl carbonate and its implementation in a full-cycle process to recycle both the polyol and the aromatic precursors. (b) Equilibrium between carbonate, carbamate and urea functional groups, as a model for the bond cleavage in PUF with a carbonate. (c) Illustration of the depolymerization and product workup of PUF depolymerization with diethyl carbonate; reaction in an autoclave at 210 °C for 4 h. <sup>1</sup>H NMR spectra are recorded in a 1 : 4 (v/v) CDCl<sub>3</sub> : DMSO-*d*<sub>6</sub> mixture.

polyol and aromatic monomers were present in the liquid phase. The sole presence of the characteristic aromatic peaks of the 2,4-/2,6-TDC monomers (Fig. 2c and Table S2) shows that no mono-carbamates or diamines remain after the reaction. Additionally, the characteristic signal at 1.04 ppm of the methyl protons in the propylene oxide (PO) units confirms the presence of the polyol in the liquid phase. The ethyl peaks at 1.25 ppm and 4.20 ppm show that the polyol has reacted with excess DEC and has become functionalized by carbonate end groups (Fig. S1). The DOSY NMR shows that the polyol was the largest compound (molecular weight-wise) in the liquid phase (Fig. S2), as witnessed by the slowest diffusion coefficients of

the polyol in comparison to TDC. In the main reaction shown in Fig. 2b and c (full spectrum shown in Fig. S3), the liquid product represented a recovery of 80% of the aromatic components, 70% as 2,4- and 2,6-TDC and the remaining 10% as putative oligomeric products, alongside a 90% of the carbonated polyol (as demonstrated in Fig. 2a).

Control experiments confirmed that both the presence of the Zn acetate catalyst and the excess of DEC, without additional nucleophile, are important to achieve the formation of aromatic dicarbamates. For the first thermal control, *i.e.*, PUF depolymerization with only DEC without catalyst (Fig. 2d), the mixture of products was insufficiently resolved to



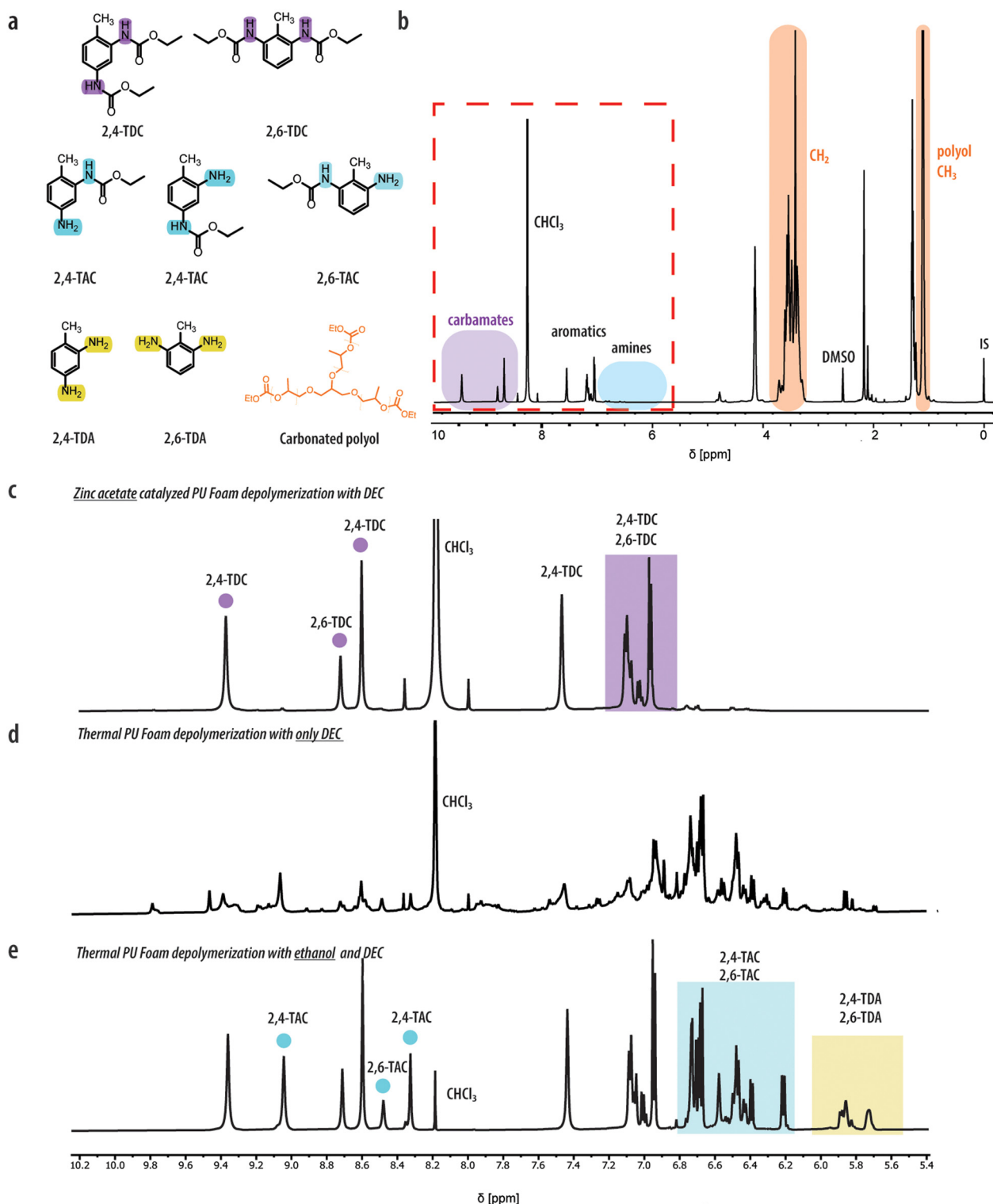


**Fig. 2** Characterization of the liquid phase after PU depolymerization: (a) PUF depolymerization products.  $^1\text{H}$  NMR spectra (recorded in 1 : 4 (v/v)  $\text{CDCl}_3 : \text{DMSO}-d_6$  mixture) of the filtrate after separation of the solid fraction: (b) in a typical experiment with 0.4 g foam, 20 mL DEC and 20 mg  $\text{Zn}(\text{OAc})_2$ , without ethanol; (c) partial spectrum of B focusing on the aromatic region; (d) same region for the thermal, uncatalyzed PUF depolymerization with only DEC (0.4 g foam and 20 mL DEC); (e) same region for the PUF depolymerization with the cosolvent ethanol (0.2 g of foam, 4 : 6 ethanol : DEC ratio with a total of 10 mL), without  $\text{Zn}(\text{OAc})_2$ .

quantify each monomer separately. The signals between 5.60 and 7.60 ppm were assigned to the aryl protons of all aromatics that originate from the same 2,4/2,6-TDI precursors. Taking the full integral of the toluene methyl signals resulted in a 60% aromatic yield with an unknown mixture of aromatic monomeric units. In Fig. S4 the DOSY NMR spectrum of the reaction revealed comparatively slower diffusion constants for the aromatic monomers, closer to that of the polyol, which indicates the possibility of residual oligomeric urea blocks. A possible reason for the incomplete depolymerization might be the poor accessibility of the urea bonds in a well-packed aromatic domain that limits the interactions with the DEC. To support this idea, we investigated the presence of a more polar co-solvent for PUF depolymerization by adding some ethanol to the DEC, still in the absence of catalyst. The conversion was improved and the liquid product contained aromatic monomers. Fig. 2e shows the appearance of peaks characteristic of mono-carbamates and diamines, including 20–30% of toluene diamines TDA together with toluene-aminocarbamates TAC and -dicarbamates TDC (Fig. S5). To further test alcoholysis in the absence of DEC, we conducted a depolymerization experiment using only ethanol (Fig. S6). This experiment yielded 60% of aromatics, resulting in significant aromatic amine by-products. Overall, these control experiments indicate that zinc acetate, acting as a Lewis acid catalyst, facilitates the carbonyl exchange reaction, and that performing the reaction in absence of nucleophile (*i.e.*, with only DEC without additional alcohol) provides primarily carbonated polyol and aromatic dicarbamates, which is distinctly different from known alcoholysis and hydrolysis processes.

Analysis of the small amount of remaining solid showed primarily some aromatic oligomers and the majority of the Zn, but no polyol (Fig. S7a). The broad signals between 6–10 ppm in the  $^1\text{H}$  NMR spectrum of the solid dissolved in  $\text{DMSO}-d_6$ , as shown in Fig. S7b, indicate the presence of oligomeric aromatic products. The FT-IR spectrum of the solid sample (Fig. S8) shows the disappearance of the characteristic polyether polyol peaks at  $1109\text{ cm}^{-1}$  (aliphatic ether group stretching)<sup>33</sup> and  $1736\text{ cm}^{-1}$  (C–O stretching of urethane groups),<sup>33,34</sup> which proves the cleavage of urethane bonds between polyol and aromatics. Additionally, the zinc contents of the solid and liquid fractions were analyzed by elemental analysis. Table S3 shows that >90% of the zinc remains in the solid fraction, with less than 10% of the Zn present in the liquid phase. The Zn amount in the liquid phase was calculated (see Table S4) based on the total liquid mass since the samples were dissolved in a known volume of internal standard solution (TSP in  $\text{DMSO}-d_6$ ) for NMR quantification. The Zn species in the solid phase are no longer purely  $\text{Zn}(\text{OAc})_2$ , as suggested by the evidence from FT-IR and XRD analyses. FT-IR spectroscopy showed characteristic vibrations of Zn–OAc at  $1559\text{ cm}^{-1}$ ,  $1447\text{ cm}^{-1}$  and Zn–O at  $500\text{ cm}^{-1}$  in the solid residue (Fig. S9). Consistent with the findings of Li *et al.*,<sup>35</sup> XRD analysis further revealed diffraction peaks in the solid residue matching  $\text{ZnO}$  (Fig. S10), indicating the formation of  $\text{ZnO}$  alongside residual  $\text{Zn}(\text{OAc})_2$ ,  $\text{ZnO}$  and possibly other zinc complexes.<sup>36,37</sup>

## Investigation of equilibration of carbonates, carbamates and ureas

Equilibration between the carbonyl compounds – carbonates, carbamates and ureas – was confirmed by performing reactions with model compounds. We first chose the model reaction between diphenyl urea (DPU), DEC and ethyl phenyl carbamate (EPC) to explore this equilibration (Fig. 3a). The main difficulty appeared to be the control over the stoichiometric ratio of DEC to DPU/EPC, as DEC is normally the solvent as well as a reagent, and its large excess drives the reaction with DPU to the right making the reverse reaction, starting from EPC to form DPU, difficult to observe. Another complication turned out to be the formation of side-products at low DEC amounts. All possible reactions are shown in Fig. S11. These include the decomposition of DPU into aniline and phenyl isocyanate as intermediates, and the possible hydrolysis of the isocyanate (*e.g.*, by the moisture bound to the  $\text{Zn}(\text{OAc})_2$ ) to produce another equivalent of aniline. Subsequently, the formed aniline can react with excess DEC to generate the corresponding carbamate.

To study the equilibration at different DEC concentrations to lower the DEC : DPU ratio, we selected sulfolane as an inert solvent. Sulfolane has excellent thermal stability, which allows for safe operation at elevated temperatures. Additionally, its low volatility and non-flammability reduce environmental and safety risks during processing. Initial tests were subjected to

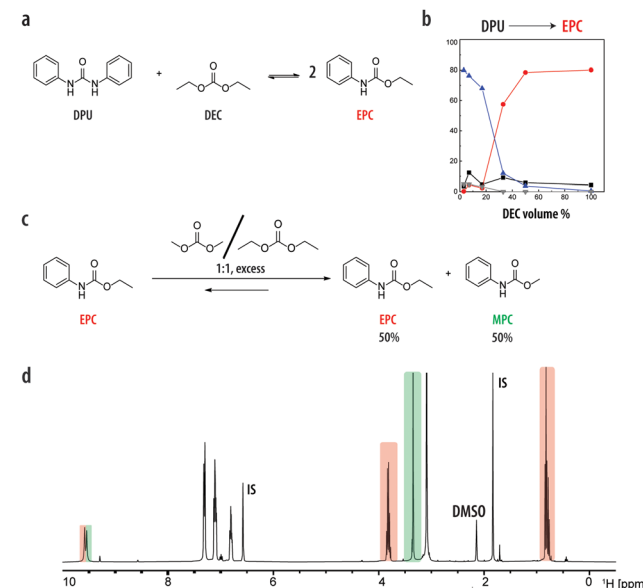


**Fig. 3** Carbonyl exchange equilibrium of model compounds *N,N*-diphenylurea (DPU) and ethyl phenyl carbamate (EPC) with DEC and  $\text{Zn}(\text{OAc})_2$  (■ DPU, ● EPC, ▲ Aniline, ▽ Biuret). (a) Schematic of the equilibrium between a urea (DPU), a carbonate (DEC) and a carbamate (EPC). (b) Relative amounts of DPU and products for reactions performed at varying DEC volume fractions for 4 h (in mixtures with sulfolane). (c) Schematic of the equilibrium between EPC, DEC/DMC and methyl phenyl carbamate (MPC). (d)  $^1\text{H}$  NMR spectrum of the compounds in  $\text{DMSO}-d_6$  after 4 h, EPC:Carbonate ratio 1:30, dimethyl carbonate (DMC):DEC ratio 1:1, 10 mg  $\text{Zn}(\text{OAc})_2$  (IS = internal standard).



conditions similar to the PUF depolymerization in DEC with Zn acetate. In a typical reaction, the crude product contained EPC and aniline besides unconverted DPU and DEC. The chemical shifts of all compounds were confirmed by comparison with the reference spectra of commercially available EPC, DPU and aniline. Fig. S12a shows the peaks we chose for qNMR, the NH signals at 9.5 ppm and 8.6 ppm of EPC and DPU, respectively, and the aryl signals at 6.5 ppm for aniline (Table S5). As expected, large amounts of DEC push the equilibrium toward EPC.<sup>26</sup> Fig. S12b shows the results of DPU conversion to EPC in sulfolane with an equal molar ratio of DPU: DEC (1:1) for 2 and 4 h, showing that aniline is the main product from the DPU decomposition already after 2 h. The reverse reaction – EPC conversion in pure sulfolane, Fig. S12c – exhibits practically complete EPC conversion in 4 h. However, hardly any DPU is formed, instead an increasing yield of aniline is observed in time, together with the formation of small amounts of 1,3,5-triphenylbiuret as a side product. Hence, we tried to reduce the amount of DEC while maintaining the total solvent volume constant through the addition of sulfolane. Fig. 3b shows the DPU conversion and product yields across varying volume fractions of DEC. Below 40% of DEC, a sharp decline in the yield of EPC was observed, while the yield of aniline continued to rise with decreasing DEC amounts. In contrast, with 50% DEC or higher, the conversion to EPC significantly improved to near-complete. A Karl Fischer titration showed the presence of  $4.72 \pm 1$  wt% (2.65 M) of water in the sulfolane. This is more than sufficient to explain the formation of all aniline at high sulfolane fractions, most likely through hydrolysis pathways.

Despite the fact that we need high amounts of DEC to suppress aniline formation, small amounts of DPU are formed when starting from EPC confirming equilibration. We tried to estimate the equilibrium constant ( $K$ ) of the reaction between DPU, EPC and DEC assuming that (i) equilibrium is reached and (ii) the preparation and cooling down times do not influence the equilibrium. Starting from DPU, the average value of  $\log K$  was 0.23, and from EPC,  $\log K$  was 0.22. These near-identical values indicate that equilibrium is indeed achieved. Moreover, there is a small preference to form EPC, and a large excess of DEC will push the equilibrium to the right.

As an additional method to support equilibration between carbonates, ureas and carbamates, we studied the scrambling of alkyl groups on a carbamate by reacting EPC with an equimolar mixture of dimethyl carbonate (DMC) and DEC, at an excess of carbonate (carbamate : carbonate ratio of 1:30; see Fig. 3c). Fig. 3d and Fig. S13 show the peaks of EPC and MPC after the reaction. The reaction led to an equal amount of EPC and methyl phenyl carbamate (MPC), confirming the equilibration between the two carbamate species.

We presume that the observed equilibration, which is promoted by Zn acetate catalysis, proceeds by action of a nucleophile on a carbonyl center to induce the exchange. Although deep mechanistic aspects are beyond the scope of this study, the observations from both the PU depolymerization and the model compound reactions indicate the intermediate liber-

ation of nucleophiles. A first observation is that the addition of ethanol does not drastically speed up the reaction, but it does change the product distribution. Secondly, leaving out the catalyst does again change mainly the product distribution, but also slows down the reaction. Thirdly, at relatively low DEC loadings, aniline becomes the major product of DPU conversion. Various nucleophiles may play a role, notably acetate from the Zn acetate catalyst, ethanol or ethanoate from DEC and aromatic amines, in part already present in the PU foam (because its formation ends with some excess of unused isocyanates which are hydrolyzed to amines, calculation shown in SI) and in part formed by urea cleavage at high temperature.

All main reaction parameters – temperature, DEC amount, catalyst amount and reaction time have a positive effect on the depolymerization process of PUF. Fig. 4a and b shows the results of temperature variation experiments conducted at 180–210 °C. The decreasing trend in residual solid weight% (Fig. 4a) with increasing temperature indicates that the hard segments within the PUF network break down to smaller compounds at elevated  $T$ . At the same time, the conversion increased with concomitant increasing yields of polyol and TDC (Fig. 4b), providing complete PUF depolymerization at 210 °C. Fig. 4c demonstrates the product yields at three different DEC:foam ratios. Interestingly, polyol yields are sig-

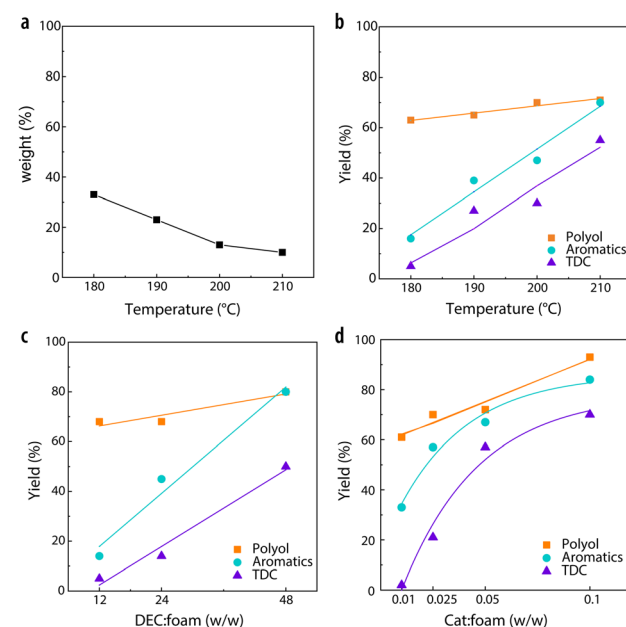


**Fig. 4** Depolymerization results of variations of temperature, concentration of DEC, and catalyst amounts. (■) Polyol, (●) Aromatics, (▲) TDC (a) Residual solid weight% (based on 0.4 g of foam) after depolymerization at 180, 190, 200 and 210 °C for 2 h. Reaction conditions: 0.4 g foam, 20 mL of DEC, 20 mg of  $Zn(OAc)_2$ . (b) Yield of polyol, aromatics, TDC at different temperatures for 2 h. Reaction conditions: 0.4 g foam, 20 mL of DEC, 20 mg of  $Zn(OAc)_2$ . (c) Yield of polyol, aromatics, and TDC at varying amounts of pure DEC for 4 h. Reaction conditions: 0.4 g foam, 20 mg of  $Zn(OAc)_2$ . (d) Yield of polyol, aromatics, and TDC at varying amounts of  $Zn(OAc)_2$  for 2 h. Reaction conditions: 0.4 g foam, 20 mL of DEC. Lines are guides to the eye.



nificantly higher compared to the aromatic yields at lower DEC amounts. Furthermore, Fig. 4d shows the influence of the  $\text{Zn}(\text{OAc})_2$  catalyst : foam ratio on the product yields. Using 10 wt% of the catalyst, the highest yields of both polyols and aromatics were achieved within 2 h, with the TDC yield up to 70%.

### Catalyst role on depolymerization of PUF

Both the Zn cation and the acetate anion appeared to be important constituents of the catalyst to achieve high reactivities and good yields of polyols and aromatics. All attempts (see Table S6) to replace either the Zn cation (by using  $\text{NaOAc}$ ) or the acetate anion (by using  $\text{ZnO}$ ,  $\text{Zn}$  stearate, zinc triflate, or  $\text{ZnCl}_2$ ), demonstrated that the original  $\text{Zn}(\text{OAc})_2$  is more effective in achieving high selectivity and yields of polyols and aromatics during PUF depolymerization.

With some pretreatment, the Zn collected in the solid fraction can be reused. To test the activity of the zinc compounds, present in the solid fraction, the entire solid was reused in place of  $\text{Zn}(\text{OAc})_2$  for a second depolymerization reaction under the same experimental conditions. Without pretreatment, we observed that the conversion of PUF into its monomers was not sufficiently high to achieve the expected aromatic yield, with a significant drop in TDC yield (<10% compared to 70% in the first cycle, Table S7). This suggests that the catalyst lost its activity after PUF depolymerization reaction, likely due to the formation of inactive Zn species. We tried to reactivate the zinc catalyst with acetic acid, as did Li *et al.*<sup>38</sup> for the reaction of dimethyl carbonate and aniline to methylene diphenyl dicarbamate (MDC). This simple process effectively restored the catalyst's activity, as shown by a significant recovery of dicarbamate yield in the second depolymerization reaction. The TDC yield improved from 10% in the untreated cycle back to above 50% after reactivation, closely aligning with the initial performance of 70% observed using fresh Zn acetate. This indicates that the reactivation process successfully resulted in dicarbamate formation, and it highlights the potential for recycling the zinc catalyst in a sustainable PUF depolymerization process.

Our approach shows the potential for full recovery of the polyol with minimal degradation. We treated the carbonated polyol with 1 M  $\text{NaOH}$  solution at 40 °C to hydrolyze the carbonate end groups that formed during the reaction (Fig. S14a). As shown in Fig. S14b, the FT-IR spectra provide clear evidence of the disappearance of the carbonyl group at 1740  $\text{cm}^{-1}$ , supporting the cleavage of carbonate from the polyol. This observation is further confirmed by  $^1\text{H}$  NMR analysis (Fig. S15), showing the disappearance of the ethyl peaks at 1.25 ppm and 4.20 ppm. The molecular weight distribution of the recovered polyol was assessed by GPC and compared to that of virgin polyol (Fig. S16). The chromatograms show a comparable polydispersity, with only a minor shift to higher molecular weight for the carbonated polyol. These findings are consistent with end-group modification. After hydrolysis, the GPC trace of the de-carbonated polyol closely resembles that of the virgin polyol, further supporting the successful recovery of the original structure. While these results validate the efficient recov-

ery of the polyol, achieving full process closure requires addressing the formed ethanol by either converting it back into DEC on-site or developing sustainable manufacturing options for DEC. Such steps would ensure system circularity and minimize the overall environmental footprint of the process.

The closure of the entire recovery process, as depicted in Fig. 1a, provides a promising pathway for a complete recovery of PUFs. However, the key steps involve the freeing of the end groups in the polyol and thermal cleavage of dicarbamate linkages. Leitner *et al.*<sup>39</sup> demonstrated a potential route for closing the aromatic loop by converting methylene phenyl carbamate into phenylisocyanate and methanol. This conversion not only closes the loop but also opens new possibilities for improved recycling efficiency, further enhancing the sustainability of the entire recovery process by eliminating the currently used industrial phosgene application.

### Applicability to post-consumer PUs

To assess the broader applicability of our method, we investigated a diverse set of pristine and post-consumer polyurethanes (PUs), including flexible foams, rigid foams and thermoplastic PU (TPU). Fig. 5 summarizes the results for six representative commercial PU and end-of-life (EoL) products: household sponges (PU-1, PU-2), a flexible foam couch (PU-4), a mattress foam (PU-5), a TPU dialysis tube (PU-3), and a memory foam insole (PU-6). These samples represent a range of PU morphologies and additive contents commonly encountered in consumer and medical waste streams.

Household kitchen sponge	EoL flexible foam couch
PU-1 257.0 mg  Liquid mass 232.0 mg  90 wt% recovery	PU-4 291.8 mg  Liquid mass 240.0 mg  82 wt% recovery
EoL household kitchen sponge	EoL flexible foam mattress
PU-2 275.7 mg  Liquid mass 251.8 mg  91 wt% recovery	PU-5 289.4 mg  Liquid mass 270.2 mg  93 wt% recovery
TPU dialysis tube (rigid PU w/ MDI)	Shoe insole (memory foam PU)
PU-3 276.7 mg  Liquid mass 253.0 mg  91 wt% recovery	PU-6 289.6 mg  Liquid mass 280.0 mg  96 wt% recovery

**Fig. 5** Depolymerization recovery results of various post-consumer PU waste types. All reactions were performed in 95 mL autoclave at 800 rpm. Recoveries are given based on liquid weight% (based on initial foam weight) after depolymerization at 210 °C for 4 h. Reaction conditions:  $\approx 0.3$  g foam, 10 mL of DEC, 10 mg of  $\text{Zn}(\text{OAc})_2$ . All samples were treated following the general procedure for PUF depolymerization described in the Experimental section.



All tested foams were successfully depolymerized in DEC with zinc acetate facilitating carbonyl exchange reaction. The process showed efficient conversion of the PU matrix into a liquid phase with minimal solid residue. Liquid mass recoveries, defined as the mass of the liquid phase relative to the mass the input foam, ranged from 80 to 96 wt%. Notably, both fresh and EoL household sponges (PU-1 and PU-2) yielded over 90 wt% recovery. The rigid TPU sample (PU-3), which differs significantly in structure and isocyanate content (MDI-based), also depolymerized in DEC, affording a 91 wt% recovery with full methylene diphenyl-4,4'-dicarbamate (MDC) formation. Lastly, the memory foam insole (PU-6), which is also MDI-based, resulted over 96 wt% recovery with minimal solid residue aside. All NMR spectra of the liquid phases are shown in the SI. These spectra show, as expected, variations of the types of peaks and their relative intensities in the aromatic and aliphatic areas, but since we did not analyze the starting compositions of these PU samples, we did not analyze these spectra further. These preliminary results collectively demonstrate that our DEC-based depolymerization method is broadly applicable across different classes of commercial PUs and PU waste, including flexible, rigid, and thermoplastic variants. This underscores the potential of the approach for real-world implementation in PU recycling.

## Conclusions

This study demonstrates the successful depolymerization of PUF in DEC using zinc acetate as a catalyst, providing an efficient pathway for recovering polyol and aromatic monomers, with minimal solid residue. Quantitative NMR analysis confirms high efficiency and selectivity of the depolymerization, with liquid product containing 80% of the aromatic compounds, 70% as TDC monomers, and 90% of the polyol, functionalized with carbonate end groups. Control experiments and characterization analyses shows the efficacy of zinc acetate as a Lewis acid catalyst, compared to alternative Zn or acetate salts.

Our findings demonstrate an effective strategy for the recovery of both polyols and aromatic precursors with minimal degradation. The polyol can be conveniently recollected by hydrolysis or alcoholysis of the carbonate end groups, while the carbamates may be converted into isocyanates thermally, without the use of toxic and wasteful phosgene. The Zn acetate catalyst can be recycled after treating the solid residue with acetic acid. The applicability of our method to diverse post-consumer PU wastes highlights its potential for practical recycling routes. An interesting alternative route may be to react the carbonated polyol and the aromatic dicarbamate directly, again in a carbonyl exchange process, to reform polyurethanes. In the future, meaningful scale-up experiments should be conducted, to account for parameters such as potential contaminants, accumulation of trace components upon recycling, heat management, product separation and purification strategies, and safety aspects, all of which require careful engineering considerations and process development.

## Experimental

### Materials and equipment

Unless otherwise stated, all reagents were purchased from commercial suppliers (Sigma-Aldrich, VWR Chemicals, Acros Organics B.V.B.A. and Shell), used without further purification and stored under ambient conditions. All the compounds down below are purchased from Sigma-Aldrich. Reagent grade diethyl carbonate (DEC, 99%), *N,N'*-diphenyl urea (DPU, 98%), ethanol (EtOH, >99.5%), 3-(trimethylsilyl)propanoic acid-*d*<sub>4</sub> sodium salt, 98 atom% D (TSP, Acros Organics B.V.B.A.), mesitylene (MS, 98%), sulfolane (99%) and zinc acetate (Zn(OAc)<sub>2</sub>, 99.99%), zinc oxide (ZnO, powder, 99.9%), zinc stearate (Zn (C<sub>18</sub>H<sub>35</sub>O<sub>2</sub>)<sub>2</sub>), zinc triflate (Zn(OTf)<sub>2</sub> 98%), zinc chloride (ZnCl<sub>2</sub>, 99%), indium acetate (In(OAc)<sub>3</sub>, 99.9%), and sodium acetate (NaOAc, 99%) were used without drying and stored under ambient conditions. Deuterated solvents were purchased from Sigma-Aldrich and used as received. Ethyl *N*-phenyl carbamate (EPC), 1,3,5-trimethylphenylbiuret, 2,4-toluenedicarbamate (2,4-TDC), 2,6-toluenedicarbamate (2,6-TDC), 2,4-tolueneaminocarbamate (2,4-TAC), and 2,6-tolueneaminocarbamate (2,6-TAC) were synthesized as described<sup>39-41</sup> and stored under ambient conditions. The model PUF and the virgin polyol (CARADOL SC48-08) were provided by Shell. Polyol is a trifunctional copolyether polyol consisting of propylene oxide (PO) and ethylene oxide (EO) repeating units, with a composition reported in Table S1. It has a hydroxyl number of 48 mg KOH per g, a molar mass of 3.5 kg mol<sup>-1</sup>. PU foam sample was composed of polyol A, an isomers mixture of 2,4- and 2,6-toluene diisocyanate (TDI) with isomer ratio of 80/20 (TDI index of 107), and water as a foaming agent to chemically produce CO<sub>2</sub>.

PUF depolymerization was carried out using a Berghof BR-300 High Pressure Reactor. Unless otherwise stated, depolymerization reactions were carried out in a 95 mL reactor made of stainless steel 316Ti, with a removable PTFE vessel. The autoclave has a thermowell for thermocouple insertion, a digital manometer for pressure read-out, screw caps and two stainless steel compression bolts for sealing the contents of the reaction well.

DPU and EPC decomposition experiments were carried out using 50 mL pressure vessels made from stainless steel alloy, designed to handle a temperature range: -10–300 °C. The reactor consists of a removable PTFE gasket, a vessel, screw cap and one stainless steel compression bolt for sealing the contents of the reaction well. Unless otherwise noted, all reactions were set up using a 40 mL PTFE inlay along with a PTFE coated magnet.

<sup>1</sup>H NMR spectra were recorded at room temperature in DMSO-*d*<sub>6</sub> and CDCl<sub>3</sub> with using a Bruker 14.1 T magnet operating at 600.16 MHz for <sup>1</sup>H, equipped with an AVANCE NEO spectrometer and a 5 mm BBO probe. All experiments were performed with temperature regulation at 25 °C and they were measured with a spectral width of 12 or 16 ppm, centered at the around 5 ppm, with 32 768 complex points, employing a 90° pulse of ~13.5 µs and a relaxation delay of 30 to 60 s, above 5 times the relaxation time T<sub>1</sub>, to ensure quantification.



The processing was performed on Bruker's Topspin software, with the one-dimensional (1D) and pseudo-two-dimensional (2D) methods being zero-filled twice, phased, and apodized with an exponential multiplication.

Chemical shifts are reported in parts per million (ppm) relative to the residual solvent signal of deuterated solvent (usually DMSO set to 2.5 ppm). Abbreviations of multiplicity patterns in NMR spectra are reported as follows: s: singlet, bs: broad singlet, d: doublet, t: triplet, q: quartet, m: multiplet, dd: double doublet. Quantitative NMR analysis was determined using 3-(trimethylsilyl)propanoic acid (TSP) and mesitylene (MS) as internal standards for PUF depolymerization and model compound reactions, as further detailed below.

For PUF depolymerization, the standard in  $\text{DMSO}-d_6$  was added to the liquid crude reaction mixture after solid filtration and solvent evaporation, without any further dilution. For model compound reactions, the standard in  $\text{DMSO}-d_6$  was added to the crude reaction mixture without any workup procedure.

Infrared spectra (FT-IR) spectra of polyol and catalysts before and after reactions were recorded in the range of 350–4000  $\text{cm}^{-1}$  on a Spectrum Two FT-IR, PerkinElmer. Absorptions are reported in wavenumber ( $\text{cm}^{-1}$ ).

Elemental analyses were carried out by The Mikroanalytisches Laboratorium Kolbe. Elemental analysis found values for zinc in solid and liquid after reaction samples are within 0.10% and 6.64%, respectively.

$\text{ZnO}$ ,  $\text{Zn(OAc)}_2$  and the solid sample compound structural characterizations were performed using X-ray powder diffraction data collected using a Bruker D8 Discover X-ray diffractometer (XRD) with a scanning range of 10 to 80.

Using a Metrohm 787 KF-Titrino, a Karl-Fischer titration was performed to calculate the water content in the sulfolane samples. A 20 mL burette of Hydralan composite 5 (5 mg water per mL) was titrated in a 3:1 (v:v) solution of methanol and dichloromethane.

Commercial flexible polyurethane foam samples were freeze-dried after cooling in liquid nitrogen for 10 min prior to SEM imaging. Foams were dried overnight under vacuum. EDX and SEM analysis using HE-SE2 detector on a Zeiss Merlin SEM were performed.

SEM data was obtained from a JSM7610F-Plus (JEOL Ltd, Tokyo, Japan). Prior to their analysis, the commercial flexible polyurethane foam were freeze dried for 2 h to remove all the water. Samples were cut to fit in the SEM holder and imaged.

### General procedure for PUF depolymerization

The carbonylation reactions were carried out in a 95 mL stainless steel Berghof BR-100 High Pressure Reactor with PTFE insert, thermowell, manometer and magnetic stirrer. In this setup, PUF pieces, solvent (diethyl carbonate and/or alcohol) and optionally a catalyst were added to the reactor. Then, the autoclave reactor was sealed, purged with argon and placed in a pre-heated aluminum block at 210 °C for 4 h at 800 rpm stirring rate. The temperature control was performed internally. Afterwards, the reactor was cooled to room temperature for 1 h, and pressure was slowly released. The reactor was opened, the thermowell was washed

with 20 mL of acetone and the content of the reactor was transferred to a beaker. The solid precipitate was filtered through a filter paper and the reaction solvent is evaporated under reduced pressure. All the crude samples in the flask were dissolved in 2 mL of 10 mM of TSP solution in  $\text{DMSO}-d_6$  and 0.5 mL of  $\text{CDCl}_3$  for the quantitative  $^1\text{H}$  NMR analysis.

### Product characterization and quantification by $^1\text{H}$ NMR spectroscopy

The contents of TDA, TAC, and TDC in the liquid samples were determined using  $^1\text{H}$  NMR spectra recorded in  $\text{DMSO}-d_6$  with an internal standard. The internal standard used in this study is 3-(trimethylsilyl)propanoic acid (TSP), chosen for its stability and chemical shift at 0 ppm in  $^1\text{H}$  NMR spectroscopy to allow separation from analytes of interest. Its use is crucial for accurate quantification and correction of any potential sample loss during PUF depolymerization analysis. The quantification was based on the signal intensities of methyl groups of the respective compounds, as detailed below:

TDA isomers:  $\delta$  1.89 ppm for 2,4-TDA and  $\delta$  1.80 ppm for 2,6-TDA.

TAC isomers:  $\delta$  1.96 and 2.00 ppm for the 2,4-TAC isomers, and  $\delta$  1.89 ppm for 2,6-TAC.

TDC isomers:  $\delta$  2.11 ppm for 2,4-TDC and  $\delta$  2.03 ppm for 2,6-TDC.

Polyol PO repeating unit:  $\delta$  1.04 ppm.

The molar content of the aromatic monomers denoted as TDC and polyol (PO) present in the liquid product were determined by calibration with TSP signal at 0 ppm, according to eqn (1):

$$M_{\text{TDX or PO}} = \frac{I_{\text{TDX or PO}}}{I_{\text{IS}}} \times \frac{N_{\text{IS}}}{N_{\text{TDX or PO}}} \times M_{\text{IS}} \times (\text{Dilution factor}). \quad (1)$$

In eqn (1),  $n_{\text{TDC or PO}}$  is the molar content of the aromatic monomer (mmol);  $I_{\text{TDX}}$  is the integral of the methyl group of aromatic monomers;  $I_{\text{IS}}$  is the integral of the internal standard (TSP) and  $N_{\text{TDX}}$  is the number of the methyl protons of aromatic monomer;  $n_{\text{IS}}$  is the molar content of the internal standard in mmol.

$$\text{Recovery of polyol (mol \%)} = \frac{n_{\text{PO}}}{n_{\text{PO}}(\text{intake})} \times 100 \quad (2)$$

$$\text{Recovery of TDC (mol \%)} = \frac{n_{\text{TDC}}}{n_{\text{TDI}}(\text{intake})} \times 100 \quad (3)$$

Polyol recovery is determined based on the molar ratio of PO found in the liquid product vs. the PO intake according to eqn (2). Aromatic recovery is calculated as the molar ratio of TDC found in the product vs. TDI intake shown in eqn (3).

### General procedure for model compound decomposition experiments

The model compound reactions were carried out in a 50 mL stainless steel reactor with PTFE insert, and magnetic stirrer. In this setup, DPU (0.235 mmol) or EPC (0.470 mmol), solvent (diethyl carbonate and/or sulfolane in varying amounts) and zinc acetate

(20 wt%, 10 mg) as a catalyst were added to the reactor. Then, the autoclave reactor was sealed, purged with argon and placed in a pre-heated aluminum block at the 210 °C for designated time at 800 rpm stirring rate. Afterwards, the reactor was cooled to room temperature for 1 h, and pressure was slowly released. The reactor was opened, and the content of the reactor was transferred to a beaker. The crude reaction mixture was dissolved in DMSO-*d*<sub>6</sub>, and samples were prepared for qNMR.

### EPC decomposition with DMC/DEC

EPC (0.302 mmol), solvents (DEC (4.12 mmol), and DMC (5.93 mmol)) and zinc acetate (20 wt%, 10 mg) as a catalyst were added to the reactor. Then, the autoclave reactor was sealed, purged with argon and placed in a pre-heated aluminum block at the 210 °C for designated time at 800 rpm stirring rate. Afterwards, the reactor was cooled to room temperature for 1 h, and pressure was slowly released. The reactor was opened, and the content of the reactor was transferred to a beaker. The crude reaction mixture was dissolved in DMSO-*d*<sub>6</sub>, and samples were prepared for qNMR. All the crude samples in the flask were dissolved in 1 mL internal standard (0.05 M mesitylene in DMSO-*d*<sub>6</sub>) filled with DMSO-*d*<sub>6</sub> till 5 mL and 0.5 mL of CDCl<sub>3</sub> for the quantitative <sup>1</sup>H NMR analysis.

The signal corresponding to the internal standard (mesitylene) at 6.75 ppm was integrated and normalized based on the number of protons present in its benzene ring. Subsequently, the integrals of the compounds of interest were compared to the signal of the IS. The molar concentration (*M*) of the compounds present in the solution was calculated by eqn (4).

$$M_{\text{DPU or EPC}} = \frac{I_{\text{DPU or EPC}}}{I_{\text{IS}}} \times \frac{N_{\text{IS}}}{N_{\text{DPU or EPC}}} \times M_{\text{IS}} \times (\text{Dilution factor}) \quad (4)$$

where *M*<sub>DPU or EPC</sub> is the molar concentration of the analyte; mol L<sup>-1</sup>; *I*<sub>DPU or EPC</sub> is the integral of the analyte signal; *I*<sub>IS</sub> is the integral of the internal standard; *N*<sub>DPU or EPC</sub> analyte is the number of analyte protons; *N*<sub>IS</sub> is the number of internal standard protons; *M*<sub>IS</sub> is the molar concentration of the internal standard, mol L<sup>-1</sup>; and dilution factor = 5.00. The conversion is calculated by eqn (5).

$$\text{Conversion (\%)} = \frac{(1 - M_{\text{DPU or EPC}})}{M_{\text{initial}}} \times 100\% \quad (5)$$

Based on the model reaction shown in Fig. 3a, 1 mol of DPU is assumed to produce 2 moles of EPC:

Therefore, the yield in mol L<sup>-1</sup> is calculated by eqn (6).

$$\text{Yield of EPC or aniline (\%)} = \frac{M_{\text{DPU initial}} \times 2 \text{ mol EPC or aniline}}{1 \text{ mol DPU}} \times 100\% \quad (6)$$

The equilibrium constant is calculated by eqn (7).

$$K = \frac{[\text{EPC}]^2}{[\text{DPU}] \times [\text{DEC}]} \quad (7)$$

where [EPC]<sup>2</sup> is the concentration of EPC, which is squared because of reaction ratio, and [DPU] and [DEC] are the concentrations of DPU and DEC respectively.

## Author contributions

Conceptualization: JPL (main), JH; methodology: JH, JPL, EH, RPM; funding acquisition: JPL (main), JH; project administration: JH, JPL; supervision: JH, JPL, WV; data curation: EH, RPM, JSH, YJ, AMG; writing – original draft: EH; writing – review & editing: EH, RPM, JSH, YJ, AMG, WV, JPL, JH.

## Conflicts of interest

There are no conflicts to declare.

## Data availability

All data supporting the findings of this study, including the characterization data, are included within the paper & SI, and the raw data will be made available by the authors upon request.

Supplementary information is available. Supplementary characterization in Fig. S1 to S16 and Tables S1 to S7, including feedstock characterization and NMR spectra for all depolymerized commercial waste PUFs. See DOI: <https://doi.org/10.1039/d5gc02533h>.

## Acknowledgements

Financial support from Shell Global Solutions International B.V. is gratefully acknowledged. We acknowledge the support of C. J. Padberg for the SEM-EDX analysis and GPC measurements, of R. Zinelli and S. Michel-Souzy for the data analysis that resulted in Fig. S16, of R. A. Valadares Barrulas for the Karl-Fischer titration experiments, and of N. D. Debera, A. S. Pels, and J. M. J. Paulusse for providing polyurethane samples.

## References

- 1 M. A. Hillmyer, The promise of plastics from plants, *Science*, 2017, **358**, 868–870.
- 2 W. Post, A. Susa, R. Blaauw, K. Molenveld and R. J. I. Knoop, A Review on the Potential and Limitations of Recyclable Thermosets for Structural Applications, *Polym. Rev.*, 2019, **60**, 359–388.
- 3 J.-P. Lange, Managing Plastics Waste-Sorting, Recycling, Disposal and Product Redesign, *ACS Sustainable Chem. Eng.*, 2021, **9**, 15722–15738.
- 4 J.-P. Lange, Towards circular carbo-chemical – the metamorphosis of petrochemicals, *Energy Environ. Sci.*, 2021, **14**, 4358.

5 'Market volume of polyurethane worldwide from 2015 to 2030 (in million metric tons)' can be found under, 2024. <https://www.statista.com/statistics/720341/global-polyurethane-market-size-forecast/>, (accessed 2025-02-19).

6 J. Lee and J. H. Kim, Performance Evaluations of Flexible Polyurethane Foams Manufactured with Castor Oil-Based Bio Polyol, *Polym. Test.*, 2023, **124**, 108069.

7 G. Rossignolo and G. Malucelli, Recycling of Polyurethanes: Where We Are and Where We Are Going To, *Green Chem.*, 2024, **26**, 1132–1152.

8 J. Dormish, H. Casselmann, A. Hoffmann, J. Krause, R. W. Albach, R. Albers, H.-G. Pirkl and H.-W. Engels, Polyurethanes: Versatile Materials and Sustainable Problem Solvers for Today's Challenges, *Angew. Chem., Int. Ed.*, 2013, **52**(3), 9422–9441.

9 P. J. Schara, T. Türel, B. Eling and Ž. Tomović, Revival of Polyester-Based Polyurethane Technology: High-Yield Monomer Recovery Using Scalable, Basic Chemical Processes, *ACS Sustainable Chem. Eng.*, 2025, **13**, 4526–4534.

10 M. Syzcher, *Syzcher's Handbook of Polyurethanes*, CRC Press, 2nd edn., 2012.

11 L. Polo Fonseca, A. Duval, E. Luna, M. Ximenis, S. De Meester, L. Avérous and H. Sardon, Reducing the Carbon Footprint of Polyurethanes by Chemical and Biological Depolymerization: Fact or Fiction?, *Curr. Opin. Green Sustainable Chem.*, 2023, **41**, 100802.

12 M. B. Johansen, B. S. Donslund, S. K. Kristensen, A. T. Lindhardt and T. Skrydstrup, Tert-Amyl Alcohol-Mediated Deconstruction of Polyurethane for Polyol and Aniline Recovery, *ACS Sustainable Chem. Eng.*, 2022, **10**, 11191–11202.

13 A. Sheel and D. Pant, Chemical Depolymerization of Polyurethane Foams via Glycolysis and Hydrolysis", in *Recycling of Polyurethane Foams*, William Andrew Publishing, 2018, pp. 67–75.

14 T. Vanbergen, I. Verlent, J. De Geeter, B. Haelterman and L. Claes, Recycling of Flexible Polyurethane Foam by Split-Phase Alcoholysis: Identification of Additives and Alcoholizing Agents to Reach Higher Efficiencies, *ChemSusChem*, 2020, **13**, 3835.

15 R. Heiran, A. Ghaderian, A. Reghunadhan, F. Sedaghati, S. Thomas and A. H. Haghghi, Glycolysis: An Efficient Route for Recycling of End of Life Polyurethane Foams, *J. Polym. Res.*, 2021, **28**, 22.

16 M. Grdadolnik, A. Drinčić, A. Oreški, O. C. Onder, P. Utroša, D. Pahovnik and E. Žagar, Insight into Chemical Recycling of Flexible Polyurethane Foams by Acidolysis, *ACS Sustainable Chem. Eng.*, 2022, **10**, 1323–1332.

17 B. Zdovc, M. Grdadolnik, D. Pahovnik and E. Žagar, Determination of End-Group Functionality of Propylene Oxide-Based Polyether Polyols Recovered from Polyurethane Foams by Chemical Recycling, *Macromolecules*, 2023, **56**, 3374–3382.

18 L. R. Mahoney, S. A. Weiner and F. C. Ferris, Hydrolysis of Polyurethane Foam Waste, *Environ. Sci. Technol.*, 1974, **8**, 135–139.

19 E. Hosgor, C.-K. Lee, N. Capra, W. Verboom, J.-P. Lange and J. Huskens, Montmorillonite K10-induced decomposition of methyl *N*-phenylcarbamate to phenylisocyanate and its prospect for recovering isocyanates from polyurethanes, *Mol. Catal.*, 2024, **556**, 113930.

20 J.-P. Lange, Sustainable development: efficiency and recycling in chemicals manufacturing, *Green Chem.*, 2002, **4**, 546–550.

21 D. Simón, A. M. Borreguero, A. de Lucas and J. F. Rodríguez, Recycling of Polyurethanes from Laboratory to Industry, a Journey towards the Sustainability, *J. Waste Manage.*, 2018, **76**, 147–171.

22 N. Gama, B. Godinho, G. Marques, R. Silva, A. Barros-Timmons and A. Ferreira, Recycling of Polyurethane by Acidolysis: The Effect of Reaction Conditions on the Properties of the Recovered Polyol, *Polymer*, 2021, **219**, 123561.

23 N. Gama, B. Godinho, G. Marques, R. Silva, A. Barros-Timmons and A. Ferreira, Recycling of Polyurethane Scraps via Acidolysis, *Chem. Eng. J.*, 2020, **395**, 125102.

24 M. Grdadolnik, B. Zdovc, A. Drinčić, O. C. Onder, P. Utroša, S. G. Ramos, E. D. Ramos, D. Pahovnik and E. Žagar, Chemical Recycling of Flexible Polyurethane Foams by Aminolysis to Recover High-Quality Polyols, *ACS Sustainable Chem. Eng.*, 2023, **29**, 10864–10873.

25 B. Liu, Z. Westman, K. Richardson, D. Lim, A. L. Stottlemeyer, T. Farmer, P. Gillis, V. Vlcek, P. Christopher and M. M. Abu-Omar, Opportunities in Closed-Loop Molecular Recycling of End-of-Life Polyurethane, *ACS Sustainable Chem. Eng.*, 2023, **11**, 6114–6128.

26 A. Ferran-Vidal, S. Wershofen, F. X. Rius-Ruiz, N. Bonet and E. Reixach, Zinc Acetates as Efficient Catalysts for the Synthesis of Bis-isocyanate Precursors, *Ind. Eng. Chem. Res.*, 2010, **49**, 6362–6366.

27 Y. Wang, X. Ding and Z. Guo, How to Get Isocyanate?, *ACS Omega*, 2024, **9**, 11168–11180.

28 S.-H. Pyo, J. H. Park, T.-S. Chang and R. Hatti-Kaul, Dimethyl carbonate as a green chemical, *Curr. Opin. Green Sustainable Chem.*, 2017, **5**, 61–66.

29 G. Fiorani, A. Perosa and M. Selva, Dimethyl carbonate: a versatile reagent for a sustainable valorization of renewables, *Green Chem.*, 2018, **20**, 288.

30 M. F. O'Neill, M. Sankar and U. Hintermair, Sustainable Synthesis of Dimethyl- and Diethyl Carbonate from CO<sub>2</sub> in Batch and Continuous Flow—Lessons from Thermodynamics and the Importance of Catalyst Stability, *ACS Sustainable Chem. Eng.*, 2022, **10**, 5243–5257.

31 K. Kohli, B. K. Sharma and C. B. Panchal, Dimethyl carbonate: Review of Synthesis Routes and Catalysts Used, *Energies*, 2022, **15**, 5133.

32 Z. Liu and Y. Ma, Chemical Recycling of Step-Growth Polymers Guided by Le Chatelier's Principle, *ACS Eng. Au*, 2024, **4**, 432–449.

33 J. Catalá, I. Guerra, J. M. García-Vargas, M. J. Ramos, M. T. García and J. F. Rodríguez, Tailor-Made Bio-Based



Non-Isocyanate Polyurethanes (NIPUs), *Polymers*, 2023, **15**, 1589.

34 J. Datta, P. Kasprzyk and K. Blazek, Diamine derivatives of dimerized fatty acids and bio-based polyether polyol as sustainable platforms for the synthesis of non-isocyanate polyurethanes, *Polymer*, 2020, **205**, 122768.

35 F. Li, X. Wang, H. Li, S. Wang, W. Xue and Y. Wang, The Induction Period of Novel Active Species in  $Zn(OAc)_2$  Catalyzed Synthesis of Aromatic Carbamates, *Catal. Lett.*, 2017, **147**, 1478–1484.

36 Z. Xia, Y. Wang, Y. Fang, Y. Wan, W. Xia and J. Sha, Understanding the Origin of Ferromagnetism in ZnO Porous Microspheres by Systematic Investigations of the Thermal Decomposition of  $Zn_5(OH)_8Ac_2 \cdot 2H_2O$  to ZnO, *J. Phys. Chem.*, 2011, **115**, 14576–14582.

37 G. Wang, D. Ma, X. Jia, X. Cui, X. Zhao and Y. Wang, In Situ Preparation of Nanometer-Scale Zinc Oxide from Zinc Acetate in the Reaction for the Synthesis of Dimethyl Toluene Dicarbamate and Its Catalytic Decomposition Performance, *Ind. Eng. Chem. Res.*, 2016, **55**, 8011–8017.

38 F. Li, H. Xu, W. Xue, Y. Wang and X. Zhao, The One-Pot Synthesis of Methylene Diphenyl-4,4'-dicarbamate, *Chem. Eng. Sci.*, 2015, **135**, 217–222.

39 W. Leitner, G. Francio, M. Scott, C. Westhues, J. Langanke, M. Lansing, C. Hussong and E. Erdkamp, Chemical Utilization of  $CO_2$  in the Production of Isocyanates, *Chem. Ing. Tech.*, 2018, **90**, 1504–1512.

40 Z. Liu, Z. Fang, N. Zheng, K. Yang, Z. Sun, S. Li, W. Li, J. Wu and T. Xie, Chemical upcycling of commodity thermoset polyurethane foams towards high-performance 3D photo-printing resins, *Nat. Chem.*, 2023, **15**, 1773–1779.

41 J. S. Martin, C. J. MacKenzie, D. Fletcher and I. H. Gilbert, Characterising covalent warhead reactivity, *Bioorg. Med. Chem.*, 2019, **27**, 2066–2074.

